Precision Editing of Cyclophilin A Generates Cyclosporine and Voclosporin Resistant Cellular Therapies

Running Title: CNI-Resistant Immune Effector Cells

Holly Wobma[1,2], Francesca Alvarez Calderon[2-4], Jiayi Dong[2,3], Kayleigh Omdahl[2,3], Xianliang Rui[3], Elisa J. Rojas Palato[3], Rene S. Bermea[2,5], Alexandre Albanese[3], Franziska Wachter[2-4], Marlana Winschel[3], Katherine A. Michaelis[1,2], Lorenzo Cagnin[3], Victor Tkachev[2,6], Susan E. Prockop[2-4], Peter A. Nigrovic[1,2,7], Bruce R. Blazar[8], Ulrike Gerdemann[2-4]* and Leslie S. Kean[2-4]*

[1] Division of Immunology, Boston Children's Hospital, Boston, MA
[2] Harvard Medical School, Boston, MA
[3] Division of Hematology/Oncology, Boston Children's Hospital, Boston, MA
[4] Department of Pediatric Oncology, Dana-Farber Cancer Institute, Boston, MA
[5] Lung Transplant Program, Division of Pulmonary and Critical Care Medicine, Massachusetts General Hospital, Boston, MA
[6] Center for Transplantation Sciences, Massachusetts General Hospital, Boston, MA
[7] Division of Rheumatology, Inflammation, and Immunity, Brigham and Women's Hospital, Boston, MA
[8] Division of Pediatric Blood & Marrow Transplantation & Cellular Therapy, University of Minnesota, Minneapolis, MN

*co-senior author

Corresponding Author:

Leslie Kean, MD, PhD

Leslie.Kean@childrens.harvard.edu

Karp Research Building, 8th Floor, Room 08215

Phone: 617-919-1370

Abstract word count: 247

Main text word count: 4000

Figure count: 6

Reference count: 60

Scientific Category: Immunobiology and Immunotherapy

For original data, please contact leslie.kean@childrens.harvard.edu

Key Points

- CRISPR editing of the last exon of *PPIA* retains CypA expression but with an altered C-terminus that disrupts CsA and VCS interactions
- *PPIA*$^{\Delta C}$ immune effector cells demonstrate retained proliferation and function in the presence of CsA and VCS

Abstract

Patients who are recipients of allogeneic transplants or have underlying autoimmune disease require immune suppression, often with calcineurin inhibitors (CNI). There is an expanding repertoire of immune effector cell (IEC) therapies, including CD19 CAR-T cells and viral-specific T cells (VSTs), deployed in these patients; however, ongoing CNI therapy may be detrimental to IEC function. We thus developed a CRISPR/Cas9-based approach to engineer dual CNI [cyclosporine (CsA) and voclosporin (VCS)] resistant IEC therapies by targeting *PPIA* (encoding cyclophilin A - CypA), a critical binding partner for both drugs. Because CypA has several homeostatic functions in T cells, a complete CypA knock-out could impair cell viability. To avoid this, we edited the last exon of the *PPIA* gene, corresponding to the C-terminus of CypA, selectively disrupting amino acids that mediate CsA/VCS-based inhibition, while leaving the majority of CypA intact. Unlike an edit in an upstream exon, which was detrimental to cell survival and rapidly selected out, C-terminal editing was stable throughout expansion and preserved CypA protein expression. This edit was then introduced into two types of IECs. Edited CD19 CAR-T cells retained *in vitro* effector function in the presence of CsA/VCS, including preserved proliferation, target cell killing, and cytokine production. Edited CMV-specific T cells demonstrated antigen-specific proliferation and cytokine production in the presence of CsA/VCS. This report of site-specific CypA modification offers a promising avenue for developing next-generation IECs that should function effectively in patients receiving CsA/VCS and thus expand applications for adoptive cell therapies in multiple clinical settings.

Introduction

Immunosuppression is the cornerstone of management of allo- and auto-immunity. Calcineurin inhibitors (CNIs) are a key medication class used to prevent graft-vs-host-disease after hematopoietic cell transplantation (HCT),[1] to prevent graft rejection after solid organ transplantation (SOT),[2] and to treat autoimmune disease.[3] Standard CNIs include cyclosporine (CsA) and tacrolimus, both widely used in HCT and SOT. Next-generation CNIs with more favorable pharmacokinetic properties are also being developed, including the CsA derivative, voclosporin (VCS), which is FDA approved for patients with lupus nephritis, expanding application of this medication class.[4]

A key attribute of CNIs is their ability to inhibit lymphocyte proliferation, persistence, and function. While these characteristics form the basis of their efficacy, they can be disadvantageous for patients with allo- or auto-immune disease experiencing complications such as relapse and infection, who are increasingly being treated with adoptive immune effector cells (IEC). These IECs include chimeric antigen receptor (CAR)-T cells and viral-specific T cells (VSTs), each of which may be inhibitable by CNIs. Managing the delivery of IECs in these patients is complex, as there is a risk of flare of allo- or autoimmunity with CNI withdrawal.[5] CNI-resistance is one way to optimize the potential of IEC therapies.

Calcineurin is a phosphatase that becomes active with binding of calcium/calmodulin following T cell receptor (TCR) activation. Calcineurin mediates T cell activity in two ways: 1) it dephosphorylates the transcription factor NFAT, which can then enter the nucleus and induce pro-inflammatory cytokine gene expression,[6] and 2) it removes an inhibitory phosphate from LCK that initiates TCR signaling and maintains T cell homeostasis.[7] Additionally, calcineurin dephosphorylates synaptopodin in the kidney, resulting in podocyte instability and increased proteinuria in lupus.[8] Thus, the therapeutic benefit of CNIs derives from inhibition of T cell activation and cytokine production, with disease- and organ-specific effects also observed.

CNIs rely on immunophilins to bind calcineurin and exert their inhibitory effect. Immunophilins are a family of peptidyl-prolyl isomerases that are highly evolutionarily conserved and widely expressed.[9] They can be divided into 'FK506 binding proteins' (FKBP) and cyclophilins. Since tacrolimus and CsA/VCS can bind to calcineurin only after pairing with FKBP12 and Cyclophilin A (CypA), respectively,[10] eliminating their expression represents a potentially important approach for engineering CNI resistance. Indeed, tacrolimus resistance has been achieved by knocking-out FKBP12.[11-15] However, this knock-out also impacts the mTOR pathway, conferring resistance to rapamycin that is inseparable from resistance to tacrolimus. Unlike for FKBP12, knock-out of CypA in T cells has not been reported. This is likely due to the widespread homeostatic function of CypA such that complete deletion may be incompatible with T cell survival and function.[16-18]

To engineer CsA/VCS-resistant IECs, we employed selective CRISPR-Cas9 editing to induce a frameshift in the last exon of *PPIA,* thereby disrupting the inhibitory effect of CNIs on calcineurin while leaving the core CypA structure intact. Here, we demonstrate this targeted approach leads to resistance to both CsA and VCS in otherwise fully functional CAR-T cells and VSTs.

Methods

Immune Cell Isolation

Peripheral blood mononuclear cells (PBMCs) were isolated from healthy human donors (n = 10) using a Ficoll gradient. A Pan-T cell isolation kit (Miltenyi) was used to isolate T cells. Cells were cultured in X-VIVO15 (Lonza) media supplemented with 10% fetal bovine serum, 1% penicillin/streptomycin, 2 mM of Glutamax, and 50 μM β-mercaptoethanol. IL-2 (R&D) was added at 100 IU/mL for initial T-cell stimulation with 1:1 anti-CD3/28 Dynabeads (Gibco) and lowered to 25 IU/mL once Dynabeads were removed. No cytokines were added during functional assays.

CAR-T Production

Plasmids encoding lentiviral constructs for CD19-CD28-CD3ζ and CD19-41BB-CD3ζ CARs were designed through VectorBuilder. Viral packaging was performed as described.[19] Isolated T cells were stimulated with anti-CD3/CD28 Dynabeads for 2 days prior to transduction. Transduction was performed via spinoculation using Lentiboost (Mayflower Bioscience).[19]

Viral-Specific T Cell Production

PBMCs from HLA-A*0201 bearing CMV seropositive donors (n=3) were resuspended with 50 ng/million cells of pp65 PepMix (JPT). After a 60-minute incubation, cells were plated at 1 million cells/mL in a 24-well plate in media containing IL-4 and IL-7 (R&D; both at 10 ng/mL).[20] Fresh media and cytokines were provided every three days. CMV specificity of expanded CD8+ T cells was assessed using the HLA-A*0201-specific dextramer NLVPMVATV (Immudex).

CRISPR/Cas9 Editing

T cells were CRISPR/Cas9 edited after two days of anti-CD3/CD28 Dynabead stimulation, and CAR-T cells were edited two days after lentiviral transduction. CMV-pp65 peptide stimulated PBMCs were edited three days after exposure to pp65 PepMix. CRISPR/Cas9 editing was performed as described.[21] Guide RNAs (gRNA) were made by combining tracr RNA (IDT) with negative control cRNA (IDT) or cRNAs for *PPIA* (Exon 4: ATCCTAAAGCATACGGGTCC; Exon 5: GTGTTTGGCAAAGTGAAAGA). DNA was sequenced by Genewiz. Synthego ICE Analysis v3.0 was used to determine editing efficiency.

DNA and Protein Modelling

Frameshift variants were aligned in TCoffee[22] and viewed using Mview.[23] Structural predictions were made using AlphaFold Colab,[24] with pdb sequences compared to wildtype CypA (PDB:3k0m), viewed in Pymol v.2.5.5.

CypA Protein Validation

For flow cytometry, cells were fixed with BD Cytofix/Cytoperm and stained with CoraLite®594-conjugated CypA monoclonal antibody (Proteintech; 1:50). For Western blot, membranes were labelled with rabbit CypA polyclonal antibody (1:1000; Fisher; PA1-025) followed by an anti-rabbit HRP secondary antibody (1:5000) using 3% BSA blocking buffer. The membrane was stripped and re-stained with actin polyclonal antibody (PA5-78715).

RNA-seq

T cells from day 6 after CRISPR editing were CD8 selected (Miltenyi). Cells were kept unstimulated or re-stimulated with anti-CD3/CD28 beads for 4 hours and processed for bulk RNA-seq. Paired-end next generation sequencing was performed using the Illumina HiSeq platform. Adapter and other Illumina-specific sequences were trimmed using the Trimmomatic package (v0.39).[25] An alignment index was created using the Kallisto package (v0.50.1)[26] and the GRCh38 cDNA reference transcriptome. Only “protein coding” and “miRNA” transcripts were retained. Transcripts were normalized to 10,000 counts/sample and transformed with the “numpy.log1p” function.[27] Clustermaps were created via the Seaborn package (v0.13.2) with the linkage method set to “average” and distance set to “Euclidean”.[28]

Drug Preparation

CsA and VCS (Millipore-Sigma) powders were reconstituted in dimethyl sulfoxide and diluted for *in vitro* assays. Tacrolimus (Prograf 5mg/mL) and rapamycin (LC laboratories) were also used for *in vitro* assays. SandImmune® (Novartis) was used for *in vivo* proliferation assays.

Mixed Lymphocyte Reaction (MLR)

CRISPR/Cas9 edited T cell 'responders' were labelled with Cell Trace Violet (CTV; Thermofisher) per manufacturer's instructions (modification: 1 μL/10 million cells). In a 96-well U-bottom plate, 100,000 edited responder T cells were plated with 300,000 HLA-A*02 disparate, irradiated (30 Gy) 'stimulator' PBMCs in a total volume of 200 μL. Cyclosporine, voclosporin, tacrolimus, and rapamycin were added at indicated doses. Assays were read on day 5 after staining for CD4 (L200), CD8 (RPA-T8), and HLA-A*02 (BB7.2). The %suppression by drug was calculated by 100% $\times$ $(1 - \frac{divided_{drug}}{divided_{no\ drug}})$.[29]

CAR-T and VST Proliferation Assays

Edited CAR-T cells, 10-12 days after initial stimulation, were stained with CTV and co-cultured with a CD19 positive NALM-6 (ATCC) line knocked-out for Beta-2-microglobulin[19] to focus on CAR-driven proliferation (vs. TCR driven allo-proliferation). Cells were collected for analysis on day 3. Edited VSTs were kept in culture for 10-12 days after initial stimulation, then labeled with CTV, and re-stimulated by co-culture with pp65 PepMix loaded onto autologous PHA blasts. Samples were collected for analysis on day 4.

CAR-T Cytotoxicity Assay

Edited CAR-T cells were co-cultured with NALM6 cells for 4 hours after which co-cultured cells were stained with CellEvent™ Caspase-3/7 (Thermofisher), Zombie Aqua (Biolegend), and anti-CD19 antibody (HIB19) plus Precision Counting Beads (Biolegend). The number of live, CD19+ cells (normalized to counting beads) was used to calculate %killing based on 100% $\times$ $(1 - \frac{NALM6_{coculture}}{NALM6_{alone}})$. Cyclosporine exposed groups were precultured with drug for 48 hours prior to the assay.

CAR-T and VST Cytokine Stimulation Assay

Protein Transport Inhibitor Cocktail (eBioscience) was added to prevent cytokine secretion. For stimulation, either pp65 pepMix was added (for VSTs), NALM6 cells (for CAR-T), or PMA/ionomycin as part of the Cell Stimulation Cocktail (eBioscience; for both VST & CAR-T cells). Intracellular staining was performed after 4 hours using: FITC-anti-human TNF-α (Mab11), BV421-anti-human IL-2 (MQ1-17H12), and BV711-anti-Human IFN-γ (B27). 25 ng/mL of CsA was added for VST assays and 100 ng/mL for CAR-T cell assays. The %suppression was calculated as 100% $\times$ $(1 - \frac{\%postive_{drug}}{\%postive_{no\ drug}})$ for each cytokine.

In Vivo Proliferation Model

Animal studies were approved by an institutional IACUC. Healthy female NSG mice (NOD.Cg-Prkdc^{scid} Il2rg^{tm1Wjl}/SzJ) were injected by tail vein with 5×10^5 CD19+ NALM-6 tumor cells on Day -4 and 6×10^5 CD19 targeted CAR-T cells on Day 0 after initial labelling with CTV. 12.5 mg/kg CsA (or PBS) was subcutaneously injected daily starting on Day -2. On Day +4, blood samples were collected via retro-orbital bleed and stained for murine and human CD45 to assess for cell division. The %suppression by drug was calculated by 100% $\times$ $(1 - \frac{Geometric\ Mean\ CTV_{no\ drug}}{Geometric\ Mean\ CTV_{drug}})$.

Data Analysis

Flow cytometry data were analyzed using FlowJo v.10.7.1. Data were graphed using GraphPad Prism v.9, and statistical analysis performed with two-way ANOVA with multiple comparisons.

Results

C-Terminal PPIA editing retains CypA expression

We selectively disrupted the C-terminal region of CypA, which is critical for the interaction of CsA/VCS-CypA with calcineurin A and thus the inhibitory effect of CNIs.[30] This was achieved via targeted CRISPR/Cas9 editing of the last exon (Exon 5) of *PPIA* (**Fig. 1A**), a strategy that

maintained CypA protein expression and T cell viability. As a comparator, we edited the immediate upstream exon (Exon 4, **Fig. 1A**), an approach predicted to lead to complete gene knock-out (NMDetective-A[31] score 0.78, with scores >0.52 corresponding to translation products predicted to undergo non-sense mediated decay (NMD)).[31] With the Exon 4 edit, we observed high levels of early cell death compared to controls (**Fig. 1B)**, rapid loss of the edited T cells during cell culture **(Fig. 1C),** and consequently, minimal proliferation of edited cells **(Fig. 1D).** Notably, the Exon 5 approach was associated with a low NMDetective-A score (0.23), low early cell death, and comparable growth kinetics to *PPIA*^{WT} cells **(Fig. 1B-D)**. Henceforth, we referred to cells with the Exon 5 edit as '*PPIA*$^{\Delta C}$'.

PPIA$^{\Delta C}$ cells demonstrated a high editing efficiency when measured on Day 3 (89.5 $\pm$ 1.3%), predominantly comprised of +1 base pair (bp) and -1 bp indels (**Fig. 2A**). Edited cells demonstrated a stable editing efficiency and indel distribution over 3-4 weeks in culture (**Fig. 2B**), indicating no long-term survival disadvantage. As hypothesized, CypA protein expression was preserved when assessed at day 10, as demonstrated by flow cytometry and Western blot (**Fig. 2C-D, Suppl. Fig. 1A**)**.** To confirm long term protein expression with the +1 bp indel, Jurkat cells were CRISPR-edited, and single cell colonies were picked for the +1 bp indel. Cells expanded for >8 weeks in culture demonstrated preserved editing efficiency (98% +1 bp indel) and CypA protein expression (**Suppl. Fig. 1B**).

Based on the two predominant indels, we modeled predicted *PPIA*$^{\Delta C}$ protein structures using AlphaFold Colab[24,32] and aligned them with the wildtype protein (*PPIA*^{WT} shown in purple; **Fig. 2E**). As expected, the two predicted *PPIA*$^{\Delta C}$ protein structures align around important residues for CypA function (pink)[30,33] but vary near Arg148 (green),[30] an amino acid critical for the interaction of CypA with the CsA-calcineurin complex.[30] For the +1 bp indel protein, the regional loss of structural homology was due to a frameshift after amino acid 132, with the protein only minimally truncated (159 amino acids vs. wildtype of 165). For the -1 bp indel, the

frameshift led to a premature stop codon at amino acid 135 and thus a protein truncated prior to Arg148.

To verify that cells with *PPIA*$^{\Delta C}$ retained their baseline transcriptional landscape as well as functional TCR signaling pathways – critical for any IEC therapy – we performed RNA-seq on purified CD8+ T cells expressing either *PPIA*^{WT} or *PPIA*$^{\Delta C}$ at baseline and upon stimulation with anti-CD3/CD28 Dynabeads. Unlike the significant transcriptional differences between edited and wildtype cells previously reported for gene-addition approaches to CsA resistance[34], the transcriptomes of the *PPIA*^{WT} and *PPIA*$^{\Delta C}$ cell populations were highly similar, with no differentially expressed genes, either at baseline or after stimulation **(Fig. 2F-G, Suppl. Fig. 2)**. This included comparable induction of NFAT pathway related genes (CCL3, CCL4, IL2, TNF-α, IFN-γ) upon stimulation in both *PPIA*^{WT} and *PPIA*$^{\Delta C}$ cells (**Fig 2G**).

PPIA$^{\Delta C}$ *T cells are resistant to CsA and VCS*

To determine whether *PPIA*$^{\Delta C}$ cells were resistant to CsA and VCS, we performed a mixed lymphocyte reaction comparing division of *PPIA*^{WT} and *PPIA*$^{\Delta C}$ responder T cells in the presence of increasing doses of each agent. As shown in **Fig. 3**, *PPIA*^{WT} responder T cells exhibited a dose-dependent suppression of proliferation, while *PPIA*$^{\Delta C}$ responder T cells were substantially resistant to CSA/VCS suppression across all doses. For example, at a dose of 25 ng/mL CsA, *PPIA*^{WT} responder CD4+ T cells demonstrated 69 $\pm$ 8% suppression of division, whereas *PPIA*$^{\Delta C}$ responder CD4+ T cells demonstrated less suppression (28 $\pm$ 12%, $p < 0.0001$). Similarly, at a dose of 10 ng/mL VCS, *PPIA*^{WT} responder CD4+ T cells demonstrated 84 $\pm$ 5% suppression of division by drug, whereas *PPIA*$^{\Delta C}$ responder CD4+ T cells demonstrated less suppression (42 $\pm$ 8% $p < 0.0001$). In contrast, and consistent with the dependency of tacrolimus and rapamycin on the alternative immunophilin, FKBP12, division of *PPIA*$^{\Delta C}$ and

PPIA^{WT} responder T cells were equally suppressible by tacrolimus and rapamycin (**Suppl. Fig. 3**).

PPIA$^{\Delta C}$ *CD19 CAR-T cells are resistant to CsA and VCS*

Having established CsA and VCS resistance in primary T cells, we next sought to validate drug resistance in representative IEC therapies, beginning with CD19 CAR-T cells. Current FDA-approved CD19 CAR-T cell products contain either 41BB or CD28 costimulatory domains (denoted BBζ and 28ζ, respectively).[35] Given their distinct signaling pathways, the ability of CsA to inhibit proliferation of BBζ and 28ζ CAR-T cells, in the absence of the *PPIA*$^{\Delta C}$ edit, was first evaluated using CD19+ NALM6 *B2M*^{KO} as stimulators. As shown in **Fig. 4**, both BBζ and 28ζ were suppressible by CsA but exhibited different drug sensitivities, with BBζ-containing cells more sensitive to CsA than 28ζ-containing cells. For example, at a low E:T ratio (1:1), in which there is one tumor cell per CAR-T cell, there was 6 $\pm$ 1% suppression of BBζ CD4+ CAR-T cell division at the lowest CsA dose (12.5 ng/mL) and 77 $\pm$ 6% suppression at the highest dose (100 ng/mL). For 28ζ CD4+ CAR-T cells at the 1:1 E:T ratio, there was no suppression at either drug dose (3 $\pm$ 4% and -6 $\pm$ 4% respectively). However, high E:T ratios (10:1) rendered the 28ζ CAR-T cell inhibitable by CsA, with 59 $\pm$ 7% suppression at a CsA dose of 25 ng/mL and 92 $\pm$ 6% suppression at a dose of 50 ng/mL. Trends were similar when CD8+ CAR-T cells were assessed (**Suppl. Fig. 4**).

In proliferation assays using CRISPR/Cas9 edited 28ζ CAR-T cells and NALM6 *B2M*^{KO} cells as stimulators (E:T 10:1), the *PPIA*$^{\Delta C}$ edit in CAR-T cells led to essentially complete resistance to CsA and VCS (**Fig. 5A-B** and **Suppl. Fig. 5).** For example, at a CsA dose of 50 ng/mL, there was 45 $\pm$ 8% suppression of division of CD4+ *PPIA*^{WT} CAR-T cells vs. 3 $\pm$ 1% suppression of *PPIA*$^{\Delta C}$ cells ($p < 0.0001$). Similar findings were shown across a dose response when cells were co-cultured with VCS – for example, at a dose of 10 ng/mL, there was 41 $\pm$ 5%

suppression of division of CD4+ *PPIA*^{WT} CAR-T cells vs. 1 $\pm$ 2% suppression of *PPIA*$^{\Delta C}$ cells ($p < 0.0001$).

We then assessed the impact of CsA on the cytotoxic potential of edited CAR T cells. *PPIA*^{WT} BBζ and 28ζ CAR-T cells demonstrated suppression of killing by CsA at the lowest E:T ratio (1:4), while *PPIA*$^{\Delta C}$ CAR-T cells demonstrated no suppression of killing with CsA (**Fig. 5C-D**). For example, BBζ *PPIA*^{WT} CAR-T cells demonstrated 20 $\pm$ 2% killing in the absence of CsA vs 5 $\pm$ 3% killing in the presence of CsA ($p = 0.02$), whereas BBζ *PPIA*$^{\Delta C}$ CAR-T cells demonstrated 22 $\pm$ 4% killing in the absence of CsA vs 28 $\pm$ 4% in the presence of CsA ($p = 0.57$). There was a similar trend with 28ζ CAR-T cells, for which *PPIA*^{WT} CAR-T cells demonstrated 27 $\pm$ 3% killing in the absence of CsA vs 15 $\pm$ 8% in the presence of CsA ($p = 0.07$), and 28ζ *PPIA*$^{\Delta C}$ CAR-T cells demonstrated 24 $\pm$ 5% killing in the absence of CsA, with no inhibition of killing (in fact, increased cytotoxicity, with 38 $\pm$ 13% killing) in the presence of drug ($p = 0.05$).

To further define the impact of drug and drug resistance on CAR-T cells, we evaluated cytokine production in response to a mitogen (PMA/ionomycin) or exposure to the CAR target (NALM6 cells). Without addition of CsA, the fraction of cytokine-producing cells was comparable between *PPIA*$^{\Delta C}$ and *PPIA*^{WT} CAR-T cells (**Suppl. Fig. 6**); however, in the presence of 100 ng/ml CsA, *PPIA*$^{\Delta C}$ CAR-T cells demonstrated sustained production of IFN-γ, TNF-α, and IL-2 when compared with *PPIA*^{WT} cells. For example, in the setting of mitogen stimulation (**Fig. 5E**), there was 38 $\pm$ 8% suppression of IFN-γ induction in *PPIA*^{WT} CD8+ T cells in the presence of CsA, and less suppression of IFN-γ in the presence of CsA for the *PPIA*$^{\Delta C}$ CAR-T cells (9 $\pm$ 4% $p < 0.0001$). Similar results were observed for TNF-α, with 80 $\pm$ 10% suppression of TNF-α induction in *PPIA*^{WT} CD8+ CAR-T cells versus 33 $\pm$ 3% ($p < 0.0001$) for the *PPIA*$^{\Delta C}$ CAR-T cells. For IL-2, (which is primarily produced by CD4+ T cells), there was 89% $\pm$ 10% suppression of IL-2 induction in *PPIA*^{WT} CD4+ CAR-T cells, versus 50 $\pm$ 13% ($p < 0.0001$) for the *PPIA*$^{\Delta C}$ CAR-T cells.

These patterns were recapitulated when edited CAR-T cells were co-cultured with NALM6 cells as a source of stimulation (**Fig. 5F**).

We also validated the ability of *PPIA*$^{\Delta C}$ CAR-T cells to proliferate in the setting of CsA *in vivo*. NSG mice were injected with a human CD19+ cell line (NALM6) to provide an antigenic stimulus (**Fig. 5G-H**). As observed *in vitro*, there was marked inhibition of division of *PPIA*^{WT} CAR-T cells in mice treated with CsA relative to mice treated with PBS (47 $\pm$ 10% inhibition), whereas there was no inhibition of division by CsA for the *PPIA*$^{\Delta C}$ CAR-T cells (-24 $\pm$ 17% inhibition, with the negative value indicating preserved expansion during the experiment, $p<0.0001$).

PPIA$^{\Delta C}$ *CMV VSTs are resistant to CsA and VCS*

Next, we evaluated the impact of the *PPIA*$^{\Delta C}$ edit on VSTs targeting the cytomegalovirus (CMV) pp65 protein.[36] As shown in **Fig. 6A**, we generated CMV/pp65 specific VSTs that were 13-18% NLV-CMV dextramer positive after a 10-day exposure to pp65 PepMix. After re-stimulation with pp65 PepMix loaded PHA blasts, *PPIA*$^{\Delta C}$ VSTs demonstrated CD8+ T cell-specific proliferation (**Fig. 6B**) that was better maintained in the presence of CsA and VCS compared to *PPIA*^{WT} cells (**Fig. 6C**). For example, for CD8+ VSTs, there was 100 $\pm$ 4% suppression of division in the *PPIA*^{WT} cells vs. 22 $\pm$ 10% suppression of division with *PPIA*$^{\Delta C}$ VSTs in the setting of 25 ng/mL CsA ($p < 0.0001$) and 101 $\pm$ 2% suppression vs. 9 $\pm$ 15%, respectively, in the setting of 5 ng/mL VCS ($p < 0.0001$). Additionally, as observed with *PPIA*$^{\Delta C}$ CAR-T cells, a higher percentage of *PPIA*$^{\Delta C}$ VSTs produced IFN-γ, TNF-α, and IL-2 when stimulated with PMA/ionomycin or pp65 PepMix with CsA present (**Fig. 6D-E**).

Discussion

Here we report a targeted CRISPR/Cas9-based approach to generate CsA- and VCS-resistant IECs by modifying the CypA protein without wholescale knock-out of *PPIA* expression. Gene

edited CD19 CAR-T cells and VSTs preserved effector and proliferative functions during CsA/VCS therapy, with important clinical implications for IEC use in immunosuppressed patients. Our approach contains the key design feature of targeting the last exon of the *PPIA* gene. This achieves two critical goals. The first is that edits in this region escape NMD, which is generally not triggered when premature stop codons are found in the last exon.[31] By avoiding NMD, we preserve translation of the majority of the CypA protein, an enzyme with several critical functions in immune cells. The second goal was to specifically induce a frameshift in the C-terminus of CypA. This region is important for the interaction of CsA-CypA with calcineurin A while being separate from the catalytic region of CypA, a domain critical for the performance of its homeostatic functions as a peptidyl-prolyl isomerase.[37]

Our approach can be contrasted with prior strategies to engineer CNI-resistant cells. A gene knock-out strategy targeting the tacrolimus- and rapamycin-dependent immunophilin, FKBP12, has been previously published.[11-15,38] A similar knock-out approach has not been published for *PPIA/*CypA. This may be due to intolerance of a full *PPIA/*CypA knock-out in T cells, given the critical homeostatic functions to which CypA contributes. Indeed, in the Genome Aggregation Database (gnomAD), which contains genetic information from >70,000 individuals, the 'probability of loss-of-function intolerance' (pLI) score (ranges from 0 to 1 with 1 being loss-of-function intolerant) is 0.98 for *PPIA*[39], implying even haploinsufficiency of this protein may be selected against in the human population. Our results with the Exon 4 editing approach were consistent with this, with negative selection of the edit in cultured T cells. Both FKBP12 and CypA are conserved proteins with homeostatic functions. Most studies have described FKBP12's role in calcium signaling in cardiomyocytes and neurons;[40,41] with its role in immunity attributed to inhibition of TGF-β signaling.[18] CypA has been demonstrated to have multiple key roles in normal T cell function: it is highly expressed in T cells and functions in protein folding, cell survival, TCR signaling, infection, and inflammation.[9,33,42-47]

An alternative approach to *PPIA* gene editing has been described, which is to disrupt CsA-CypA docking with calcineurin A by gene addition of a modified calcineurin A (mCNA).[34,48] However, a limitation observed with this strategy is that cells expressing the mCNA have disrupted downstream NFAT signaling as well as other transcriptomic differences compared to unmodified cells.[34,48] For this reason, we focused on selective gene modification of *PPIA*/CypA, to avoid the loss of viability with a total *PPIA* gene deletion and the abnormal NFAT signaling observed with the mCNA addition. As predicted, we observed preserved cell survival and expansion, with stability of the Exon 5 gene edit for >3 weeks in primary T cells, and no detrimental impact on T cell activation or calcineurin signaling.

As we consider application of the *PPIA*$^{\Delta C}$ edit to IEC therapies, the differential impact of CsA on 28ζ versus BBζ CAR-T cells deserves discussion. It has been previously demonstrated that strong CD28 co-stimulation may enable T cells to overcome CNI-based suppression, possibly due to decreased NFAT export from the nucleus and enhanced PKCθ signaling.[49-52] We confirmed this also applies to CAR-T cells, as BBζ CAR-T cells were more sensitive to CsA-mediated inhibition than 28ζ CAR-T cells. However, the latter were still sensitive to CsA when cultured with decreased tumor antigen stimulation and could be rendered resistant to CsA/VCS by the *PPIA*$^{\Delta C}$ edit. These CsA and VCS resistant CAR-T cells may be considered for post-HCT patients with early B-cell malignancy relapse, post-HCT or SOT patients with post-transplant lymphoproliferative disorder, or patients with lupus nephritis, who are increasingly treated with VCS.[53,54]

We also highlight the application of the *PPIA*$^{\Delta C}$ edit to VSTs. Viral reactivation is a leading cause of morbidity and mortality in HCT and SOT patients.[55,56] In addition to triggering organ dysfunction, there is a bidirectional relationship between viremia and graft-vs-host disease/graft rejection.[57] Reduction in immune suppression may be used to treat viral reactivation and disease, but further increases the risk of alloreactivity, and traditional antiviral therapies carry significant toxicities.[58] The demonstration of substantial clinical responses with

VSTs not resistant to immunosuppression[59,60] provides a strong rationale for the utility of VSTs to treat otherwise refractory viral diseases. The addition of CsA/VCS resistance holds the promise of increasing the proliferation, peak expansion, and cytokine production of these cells in HCT and SOT patients treated with CsA or VCS, which may further increase their efficacy.

In conclusion, we have developed a novel strategy for engineering T cell resistance to CsA and VCS. This strategy can be incorporated into diverse cellular products for patients with allo- and auto-immune disease who require ongoing immune suppression with these agents.

Acknowledgments
This work was supported by National Institutes of Health R01-HL095791 (LSK), P01-HL158504 (LSK), U19-AI051731 (LSK), the Lupus Research Alliance (LSK, PAN), P30AR070253 (PAN), R01AR073201 (PAN), R01AR075906 (PAN), R01 HL11879 (BRB), R37 AI34495 (BRB), 2P01 CA065493 (BRB), NIAID T32AI007512-36 (HW), NIH K12 Child Health Research Career Development Award (FAC), ASTCT New Investigator Award (VT), Be the Match Foundation/CIBMTR Amy Strelzer Manasevit Research Grant (VT).

Authorship Contributions
HW, FAC, UG, and LSK designed experiments. HW, JD, KO, XR, EJRP, AA, FW, MW, KAM, and LC performed research. HW, RSB, AA, FAC, UG, and LSK analyzed data. HW, UG, and LSK wrote the manuscript. All authors critically reviewed and approved the content of the manuscript.

Disclosure of Conflicts of Interest
HW, SEP, and LSK have equity in Regatta Bio. HW and LSK are inventors on a submitted (pending) patent related to the topic of this paper (PCT/US2024/054075). PAN is a consultant for Alkermes, Apollo, Century Therapeutics, Merck, Monte Rosa, Novartis, Pfizer, and has received grants from BMS and Pfizer. He holds equity in Edelweiss Immune, Inc. BRB reports research funding from Carisma Therapeutics and consulting fees from BlueRock Therapeutics, Atara Biotherapeutics, Sandoz, Legend Biotech, GentiBio Inc. and Affyxell Co., Ltd. U.G. possesses intellectual property rights related to AlloVir, including interests in royalties. SEP receives support for the conduct of clinical trials through Boston Children's Hospital from Atara, and Jasper, is an inventor of intellectual property related to development of third party viral specific T cells program with all rights assigned to Memorial Sloan Kettering Cancer Center, receives honoraria from Pierre Fabre as well as consulting fees from Atara Biotherapeutics, Ensomo, HEOR, Pierre Fabre, and VOR. She serves on the DSMB for Stanford University and NYBC. LSK is on the scientific advisory board for HiFiBio. She reports research funding from Tessera Therapeutics, EMD Serono, Gilead Pharmaceuticals, and Regeneron Pharmaceuticals. She reports consulting fees from Vertex and Santa Ana Bio. Dr. Kean reports grants and personal fees from Bristol Myers Squibb. Dr. Kean's conflict-of-interest with Bristol Myers Squibb is managed under an agreement with Harvard Medical School.

References

1. Hamilton BK. Current approaches to prevent and treat GVHD after allogeneic stem cell transplantation. *Hematology Am Soc Hematol Educ Program*. 2018;2018(1):228-235.
2. Nelson J, Alvey N, Bowman L, et al. Consensus recommendations for use of maintenance immunosuppression in solid organ transplantation: Endorsed by the American College of Clinical Pharmacy, American Society of Transplantation, and International Society for Heart and Lung Transplantation: An executive summary. *Pharmacotherapy*. 2022;42(8):594-598.
3. Rovin BH, Teng YKO, Ginzler EM, et al. Efficacy and safety of voclosporin versus placebo for lupus nephritis (AURORA 1): a double-blind, randomised, multicentre, placebo-controlled, phase 3 trial. *Lancet*. 2021;397(10289):2070-2080.
4. Abdel-Kahaar E, Keller F. Clinical pharmacokinetics and pharmacodynamics of voclosporin. *Clin Pharmacokinet*. 2023;62(5):693-703.
5. Reshef R, Vardhanabhuti S, Luskin MR, et al. Reduction of immunosuppression as initial therapy for posttransplantation lymphoproliferative disorder(★). *Am J Transplant*. 2011;11(2):336-347.

6. Martinez-Martinez S, Redondo JM. Inhibitors of the calcineurin/NFAT pathway. *Curr Med Chem*. 2004;11(8):997-1007.
7. Dutta D, Barr VA, Akpan I, et al. Recruitment of calcineurin to the TCR positively regulates T cell activation. *Nat Immunol*. 2017;18(2):196-204.
8. Faul C, Donnelly M, Merscher-Gomez S, et al. The actin cytoskeleton of kidney podocytes is a direct target of the antiproteinuric effect of cyclosporine A. *Nat Med*. 2008;14(9):931-938.
9. Nigro P, Pompilio G, Capogrossi MC. Cyclophilin A: a key player for human disease. *Cell Death Dis*. 2013;4(10):e888.
10. Breuder T, Hemenway CS, Movva NR, Cardenas ME, Heitman J. Calcineurin is essential in cyclosporin A- and FK506-sensitive yeast strains. *Proc Natl Acad Sci U S A*. 1994;91(12):5372-5376.
11. Amini L, Wagner DL, Rossler U, et al. CRISPR-Cas9-edited tacrolimus-resistant antiviral T cells for advanced adoptive immunotherapy in transplant recipients. *Mol Ther*. 2021;29(1):32-46.
12. De Angelis B, Dotti G, Quintarelli C, et al. Generation of Epstein-Barr virus-specific cytotoxic T lymphocytes resistant to the immunosuppressive drug tacrolimus (FK506). *Blood*. 2009;114(23):4784-4791.
13. Maldini CR, Messana AC, Bendet PB, et al. Immunosuppressant therapy averts rejection of allogeneic FKBP1A-disrupted CAR-T cells. *Mol Ther*. 2024;32(10):3485-3503.
14. Peter L, Wendering DJ, Schlickeiser S, et al. Tacrolimus-resistant SARS-CoV-2-specific T cell products to prevent and treat severe COVID-19 in immunosuppressed patients. *Mol Ther Methods Clin Dev*. 2022;25:52-73.
15. Dragon AC, Bonifacius A, Lienenklaus S, et al. Depletion of alloreactive B cells by drug-resistant chimeric alloantigen receptor T cells to prevent transplant rejection. *Mol Ther*. 2025.
16. Aghdasi B, Ye K, Resnick A, et al. FKBP12, the 12-kDa FK506-binding protein, is a physiologic regulator of the cell cycle. *Proc Natl Acad Sci U S A*. 2001;98(5):2425-2430.
17. Dubois S, Shou W, Haneline LS, Fleischer S, Waldmann TA, Muller JR. Distinct pathways involving the FK506-binding proteins 12 and 12.6 underlie IL-2-versus IL-15-mediated proliferation of T cells. *Proc Natl Acad Sci U S A*. 2003;100(24):14169-14174.
18. Wang T, Li BY, Danielson PD, et al. The immunophilin FKBP12 functions as a common inhibitor of the TGF beta family type I receptors. *Cell*. 1996;86(3):435-444.
19. Kaminski J, Fleming RA, Alvarez-Calderon F, et al. B-cell-directed CAR-T cell therapy activates CD8+ cytotoxic CARneg bystander T-cells in non-human primates and patients. *Blood*. 2024.
20. Papadopoulou A, Gerdemann U, Katari UL, et al. Activity of broad-spectrum T cells as treatment for AdV, EBV, CMV, BKV, and HHV6 infections after HSCT. *Sci Transl Med*. 2014;6(242):242ra283.
21. Rupp LJ, Schumann K, Roybal KT, et al. CRISPR/Cas9-mediated PD-1 disruption enhances anti-tumor efficacy of human chimeric antigen receptor T cells. *Sci Rep*. 2017;7(1):737.
22. Di Tommaso P, Moretti S, Xenarios I, et al. T-Coffee: a web server for the multiple sequence alignment of protein and RNA sequences using structural information and homology extension. *Nucleic Acids Res*. 2011;39(Web Server issue):W13-17.
23. Brown NP, Leroy C, Sander C. MView: a web-compatible database search or multiple alignment viewer. *Bioinformatics*. 1998;14(4):380-381.
24. Mirdita M, Schutze K, Moriwaki Y, Heo L, Ovchinnikov S, Steinegger M. ColabFold: making protein folding accessible to all. *Nat Methods*. 2022;19(6):679-682.
25. Bolger AM, Lohse M, Usadel B. Trimmomatic: a flexible trimmer for Illumina sequence data. *Bioinformatics*. 2014;30(15):2114-2120.

26. Bray NL, Pimentel H, Melsted P, Pachter L. Near-optimal probabilistic RNA-seq quantification. *Nat Biotechnol*. 2016;34(5):525-527.
27. Harris CR, Millman KJ, van der Walt SJ, et al. Array programming with NumPy. *Nature*. 2020;585(7825):357-362.
28. Waskom ML. seaborn: statistical data visualization. *J Open Source Softw*. 2021;6:3021.
29. Rui X, Alvarez-Calderon F, Wobma H, et al. Human OX40L-CAR-Tregs target activated antigen-presenting cells and effectively control T cell alloreactivity. *Sci Transl Med*. 2024; 16(769):eadj9331.
30. Huai Q, Kim HY, Liu Y, et al. Crystal structure of calcineurin-cyclophilin-cyclosporin shows common but distinct recognition of immunophilin-drug complexes. *Proc Natl Acad Sci U S A*. 2002;99(19):12037-12042.
31. Lindeboom RGH, Vermeulen M, Lehner B, Supek F. The impact of nonsense-mediated mRNA decay on genetic disease, gene editing and cancer immunotherapy. *Nat Genet*. 2019;51(11):1645-1651.
32. Jumper J, Evans R, Pritzel A, et al. Highly accurate protein structure prediction with AlphaFold. *Nature*. 2021;596(7873):583-589.
33. Dorfman T, Weimann A, Borsetti A, Walsh CT, Gottlinger HG. Active-site residues of cyclophilin A are crucial for its incorporation into human immunodeficiency virus type 1 virions. *J Virol*. 1997;71(9):7110-7113.
34. Zhang Y, Fang H, Wang G, et al. Cyclosporine A-resistant CAR-T cells mediate antitumour immunity in the presence of allogeneic cells. *Nat Commun*. 2023;14(1):8491.
35. Feucht J, Sadelain M. Function and evolution of the prototypic CD28zeta and 4-1BBzeta chimeric antigen receptors. *Immunooncol Technol*. 2020;8:2-11.
36. Prockop SE, Hasan A, Doubrovina E, et al. Third-party cytomegalovirus-specific T cells improved survival in refractory cytomegalovirus viremia after hematopoietic transplant. *J Clin Invest*. 2023;133(10).
37. Zydowsky LD, Etzkorn FA, Chang HY, et al. Active site mutants of human cyclophilin A separate peptidyl-prolyl isomerase activity from cyclosporin A binding and calcineurin inhibition. *Protein Sci*. 1992;1(9):1092-1099.
38. Ricciardelli I, Brewin J, Lugthart G, Albon SJ, Pule M, Amrolia PJ. Rapid generation of EBV-specific cytotoxic T lymphocytes resistant to calcineurin inhibitors for adoptive immunotherapy. *Am J Transplant*. 2013;13(12):3244-3252.
39. Chen S, Francioli LC, Goodrich JK, et al. A genomic mutational constraint map using variation in 76,156 human genomes. *Nature*. 2024;625(7993):92-100.
40. Guo T, Cornea RL, Huke S, et al. Kinetics of FKBP12.6 binding to ryanodine receptors in permeabilized cardiac myocytes and effects on Ca sparks. *Circ Res*. 2010;106(11):1743-1752.
41. Hoeffer CA, Tang W, Wong H, et al. Removal of FKBP12 enhances mTOR-Raptor interactions, LTP, memory, and perseverative/repetitive behavior. *Neuron*. 2008;60(5):832-845.
42. Anto NP, Arya AK, Muraleedharan A, et al. Cyclophilin A associates with and regulates the activity of ZAP70 in TCR/CD3-stimulated T cells. *Cell Mol Life Sci*. 2022;80(1):7.
43. Daneri-Becerra C, Valeiras B, Gallo LI, Lagadari M, Galigniana MD. Cyclophilin A is a mitochondrial factor that forms complexes with p23 - correlative evidence for an anti-apoptotic action. *J Cell Sci*. 2021;134(3).
44. Bauer K, Kretzschmar AK, Cvijic H, et al. Cyclophilins contribute to Stat3 signaling and survival of multiple myeloma cells. *Oncogene*. 2009;28(31):2784-2795.
45. Colgan J, Asmal M, Neagu M, et al. Cyclophilin A regulates TCR signal strength in CD4+ T cells via a proline-directed conformational switch in Itk. *Immunity*. 2004;21(2):189-201.
46. Maneix L, Iakova P, Lee CG, et al. Cyclophilin A supports translation of intrinsically disordered proteins and affects haematopoietic stem cell ageing. *Nat Cell Biol*. 2024;26(4):593-603.

47. Yurchenko V, Constant S, Eisenmesser E, Bukrinsky M. Cyclophilin-CD147 interactions: a new target for anti-inflammatory therapeutics. *Clin Exp Immunol*. 2010;160(3):305-317.
48. Brewin J, Mancao C, Straathof K, et al. Generation of EBV-specific cytotoxic T cells that are resistant to calcineurin inhibitors for the treatment of posttransplantation lymphoproliferative disease. *Blood*. 2009;114(23):4792-4803.
49. Isakov N, Altman A. PKC-theta-mediated signal delivery from the TCR/CD28 surface receptors. *Front Immunol*. 2012;3:273.
50. Diehn M, Alizadeh AA, Rando OJ, et al. Genomic expression programs and the integration of the CD28 costimulatory signal in T cell activation. *Proc Natl Acad Sci U S A*. 2002;99(18):11796-11801.
51. June CH, Ledbetter JA, Gillespie MM, Lindsten T, Thompson CB. T-cell proliferation involving the CD28 pathway is associated with cyclosporine-resistant interleukin 2 gene expression. *Mol Cell Biol*. 1987;7(12):4472-4481.
52. Yokosuka T, Kobayashi W, Sakata-Sogawa K, et al. Spatiotemporal regulation of T cell costimulation by TCR-CD28 microclusters and protein kinase C theta translocation. *Immunity*. 2008;29(4):589-601.
53. Dall'Era M, Kalunian K, Solomons N, et al. Comparison of a voclosporin-based triple immunosuppressive therapy to high-dose glucocorticoid-based immunosuppressive therapy: a propensity analysis of the AURA-LV and AURORA 1 studies and ALMS. *Lupus Sci Med*. 2024;11(2).
54. Arriens C, Teng YKO, Ginzler EM, et al. Update on the efficacy and safety profile of voclosporin: An integrated analysis of clinical trials in lupus nephritis. *Arthritis Care Res (Hoboken)*. 2023;75(7):1399-1408.
55. Hill JA, Mayer BT, Xie H, et al. The cumulative burden of double-stranded DNA virus detection after allogeneic HCT is associated with increased mortality. *Blood*. 2017;129(16):2316-2325.
56. Limaye AP, Bakthavatsalam R, Kim HW, et al. Impact of cytomegalovirus in organ transplant recipients in the era of antiviral prophylaxis. *Transplantation*. 2006;81(12):1645-1652.
57. Cantoni N, Hirsch HH, Khanna N, et al. Evidence for a bidirectional relationship between cytomegalovirus replication and acute graft-versus-host disease. *Biol Blood Marrow Transplant*. 2010;16(9):1309-1314.
58. Avery RK, Arav-Boger R, Marr KA, et al. Outcomes in transplant recipients treated with foscarnet for ganciclovir-resistant or refractory cytomegalovirus infection. *Transplantation*. 2016;100(10):e74-80.
59. Mahadeo KM, Baiocchi R, Beitinjaneh A, et al. Tabelecleucel for allogeneic haematopoietic stem-cell or solid organ transplant recipients with Epstein-Barr virus-positive post-transplant lymphoproliferative disease after failure of rituximab or rituximab and chemotherapy (ALLELE): a phase 3, multicentre, open-label trial. *Lancet Oncol*. 2024;25(3):376-387.
60. Haque T, Wilkie GM, Jones MM, et al. Allogeneic cytotoxic T-cell therapy for EBV-positive posttransplantation lymphoproliferative disease: results of a phase 2 multicenter clinical trial. *Blood*. 2007;110(4):1123-1131.

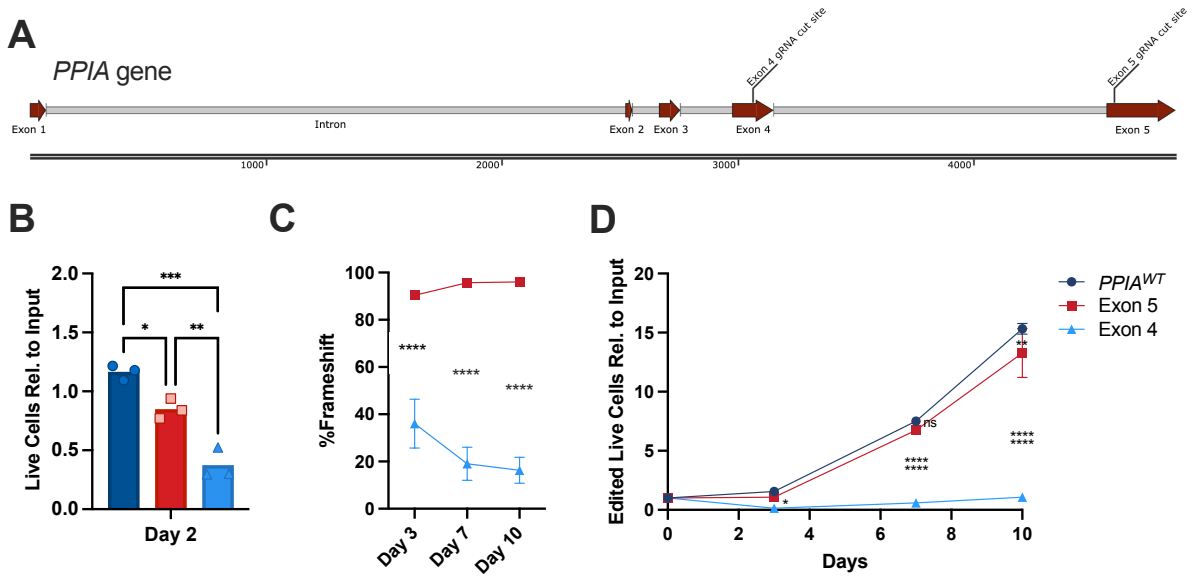

Figure 1. CRISPR/Cas9 editing of Exon 5 but not Exon 4 facilitates expansion of edited cells A) Schematic of the *PPIA* gene containing 5 exons, the largest of which are Exon 4 and Exon 5. CRISPR/Cas9 gRNA cut sites are indicated, and guide sequences are provided in the Methods. B) Significantly lower live T cell counts relative to the number of electroporated cells (input) after CRISPR/Cas9 targeting of Exon 4, two days after gene editing. Control, $PPIA^{WT}$ cells were edited with a non-targeting guide. Groups compared via One-way ANOVA with multiple comparisons. C) Change of Exon 4 and Exon 5 editing rates over time (relative to date of CRISPR/Cas9 RNP nucleofection) as determined by Sanger sequencing on Days 3 (first time point of assessing editing rate), 7 and 10. D) The degree of expansion of CRISPR-Cas9 edited cells was calculated based on the live cell count multiplied by % edited cells relative to the Day 0 input cell count. The * at Day 3 reflects the comparison between $PPIA^{WT}$ and the Exon 4 edit. The remaining Day 3 comparisons were not significantly different (ns). Experiments performed with n = 3 donors per group; data represent mean ± SD; error bars are not visible when they are smaller than the marker size.

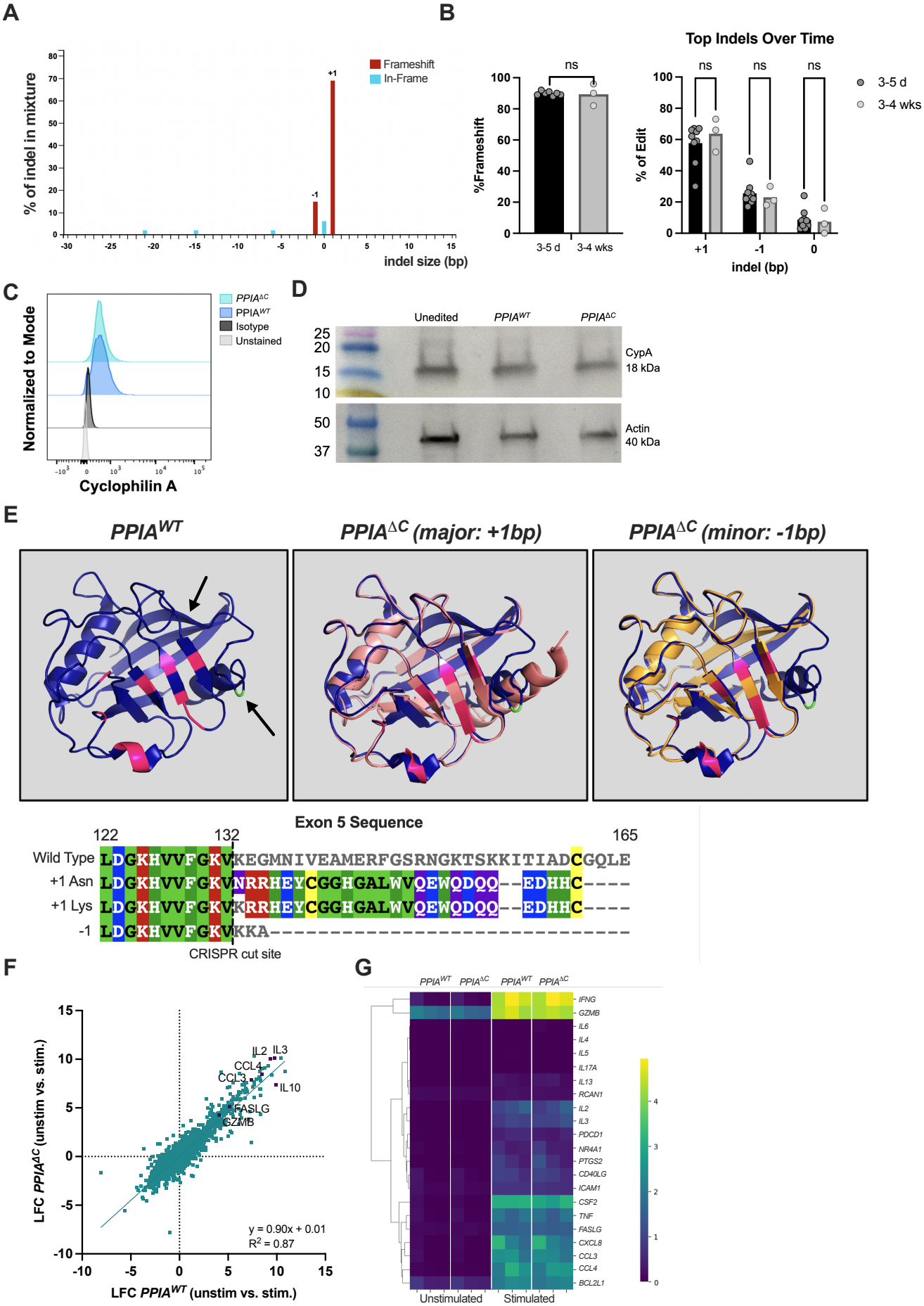
A
% of indel in mixture
Frameshift
In-Frame
+1
-1
indel size (bp)
B
Top Indels Over Time
%Frameshift
ns
3-5 d
3-4 wks
% of Edit
+1
-1
0
indel (bp)
C
Normalized to Mode
PPIA^ΔC
PPIA^WT
Isotype
Unstained
Cyclophilin A
D
Unedited
PPIA^WT
PPIA^ΔC
CypA
18 kDa
Actin
40 kDa
E
PPIA^WT
PPIA^ΔC (major: +1bp)
PPIA^ΔC (minor: -1bp)
Exon 5 Sequence
122
132
165
Wild Type
+1 Asn
+1 Lys
-1
CRISPR cut site
F
LFC PPIA^ΔC (unstim vs. stim.)
LFC PPIA^WT (unstim vs. stim.)
IL2
IL3
CCL4
CCL3
IL10
FASLG
GZMB
y = 0.90x + 0.01
R^2 = 0.87
G
PPIA^WT
PPIA^ΔC
IFNG
GZMB
IL6
IL4
IL5
IL17A
IL13
RCAN1
IL2
IL3
PDCD1
NR4A1
PTGS2
CD40LG
ICAM1
CSF2
TNF
FASLG
CXCL8
CCL3
CCL4
BCL2L1
Unstimulated
Stimulated

Figure 2. Characterizing the *PPIA*$^{\Delta C}$ edit and associated protein A) CRISPR editing at a specific locus in Exon 5 leads to a consistent indel distribution of mostly +1 > -1 bp indels. B) The overall editing efficiency and indel distribution are stable over 3-4 weeks. C-D) CypA protein expression 10 days after CRISPR/Cas9 editing by (C) flow cytometry and (D) Western blot using actin as a loading control (after stripping the membrane and re-staining) and a Precision Plus Protein™ Kaleidoscope™ ladder with corresponding protein sizes indicated on the left; no image enhancement software was used E) Predicted 3D protein structure based on AlphaFold Colab where the edited protein (rose or tangerine) is overlayed on the wildtype protein (purple). Catalytic residues important to homeostatic function are highlighted in pink (R55, F60, M61, Q63, A101, F113, W121, L122, and H126). An important residue for CsA binding is shown in green (R148; see black arrow). Another black arrow points towards a β-strand absent in the edited proteins. The corresponding amino acid sequences in Exon 5 are shown underneath as well as the CRISPR cut site after amino acid 132. F) Comparison of the log fold change (LFC) in expression (unstimulated vs. stimulated) in *PPIA*^{WT} and *PPIA*$^{\Delta C}$ CD8+ T cells, analyzed by a simple linear regression model. $p<0.0001$ G) Normalized gene expression based on bulk RNA-seq in *PPIA*^{WT} and *PPIA*$^{\Delta C}$ CD8+ T cells, highlighting genes related to TCR activation and the NFAT signaling pathway. n = 3 donors.

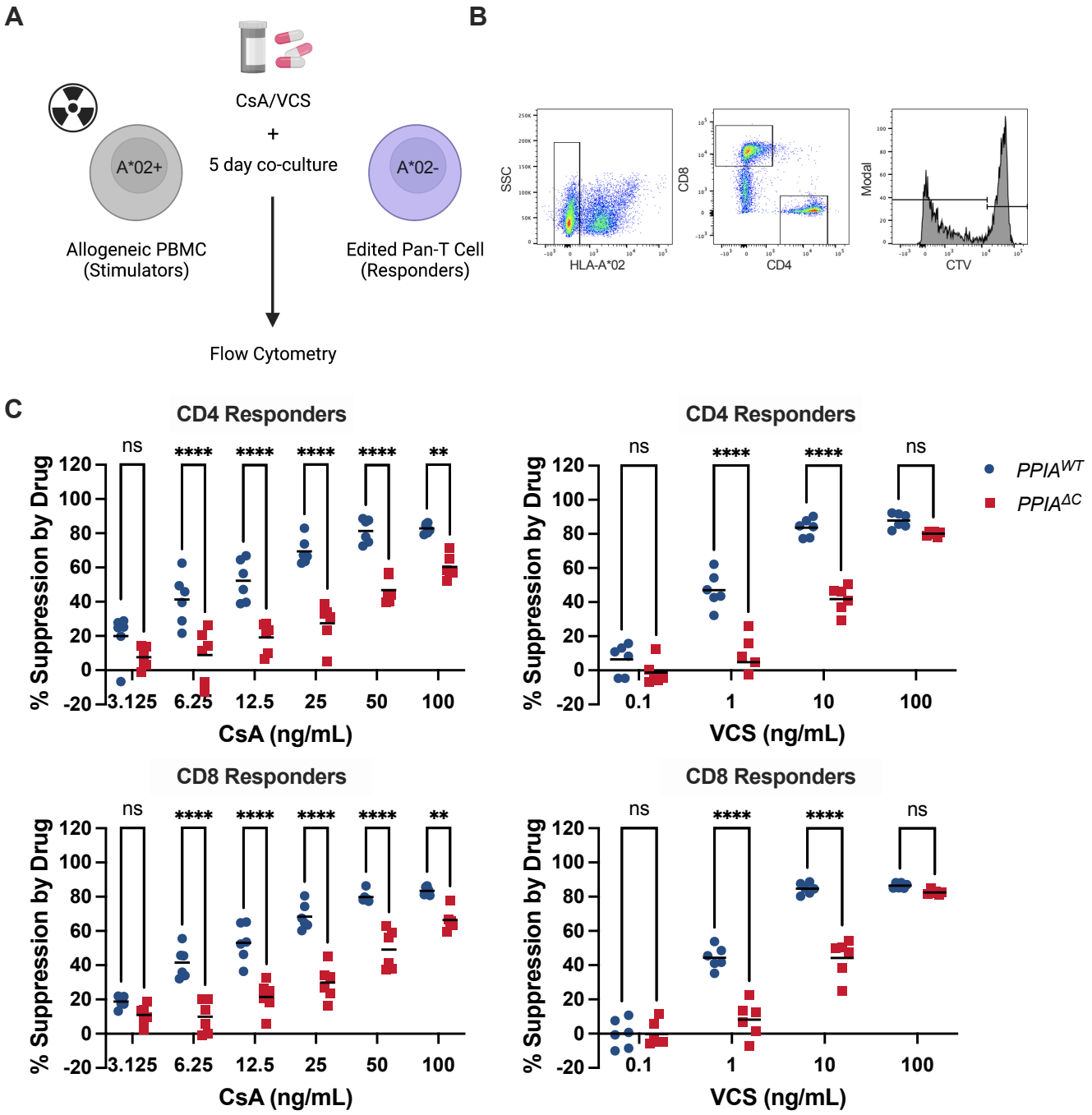

Figure 3. *PPIA*$^{\Delta C}$ T cell division is resistant to CsA and VCS suppression. A) Schematic of a mixed lymphocyte reaction suppression assay in which 'stimulator' PBMCs are in co-culture with 'responder' *PPIA*^{WT} or *PPIA*$^{\Delta C}$ T cells at a 3:1 ratio B) Gating strategy of assessing proliferating cells in the mixed lymphocyte reaction: Stimulator and responder cells were HLA-A*02 disparate allowing separation of populations on flow cytometry. Responder cells were gated on CD4+ and CD8+ T cell subsets and proliferation was evaluated based on CTV dilution within these populations. C) Division of Responder CD4+ and CD8+ T cells was assessed based on CTV dilution relative to a "Responder only" negative control group. Percent suppression by drug was calculated by normalizing data to the drug-free (positive) control (see Methods). Black bars show the mean. 2-way ANOVA with Sidak post-hoc test was used for statistical analysis. n = 6 replicates.

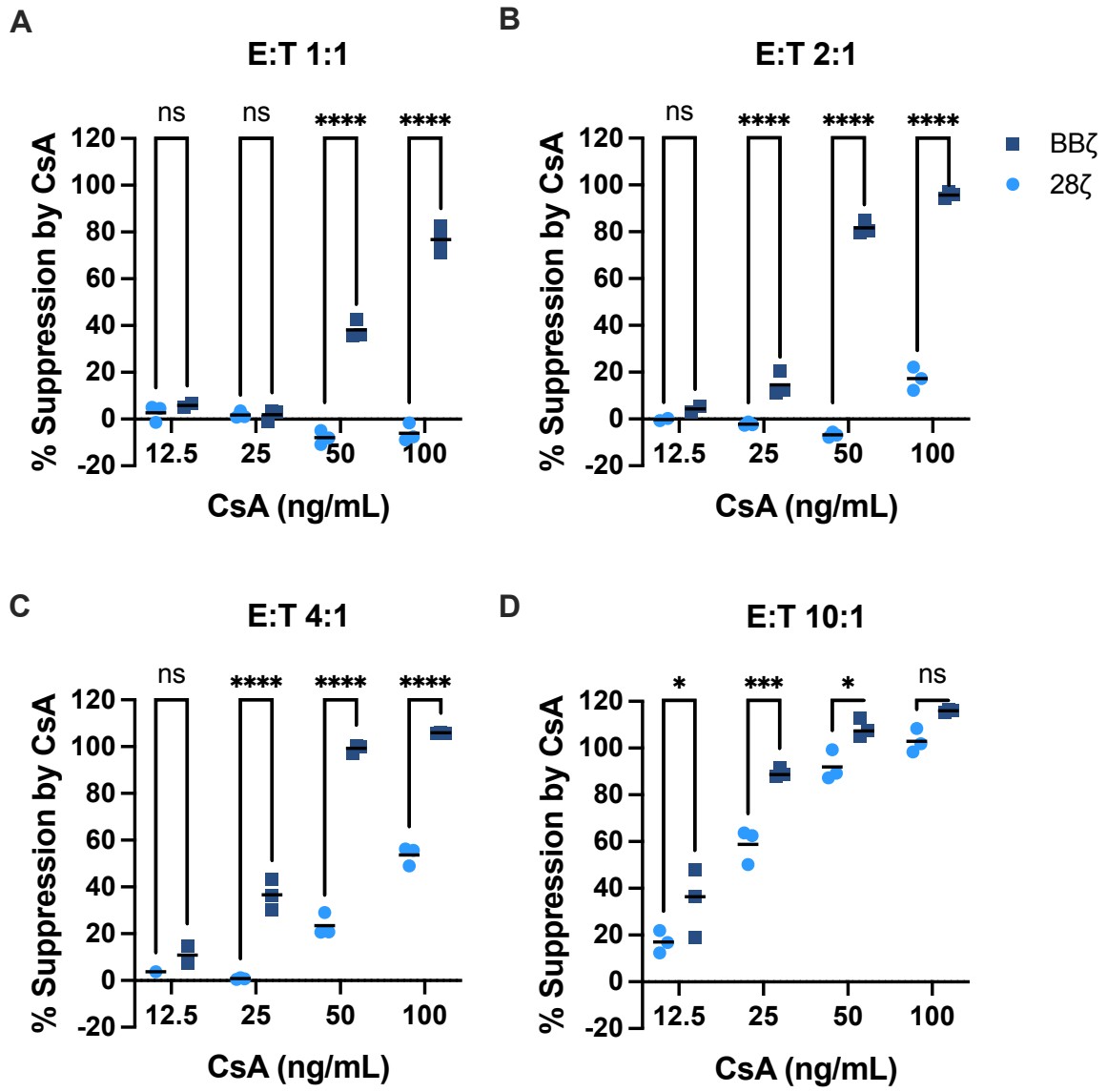

Figure 4. BBζ CAR-T cells are more sensitive to inhibition by CsA than 28ζ CAR-T cells. Division of CAR-T cells in response to CD19+ β2M^{KO} NALM6 stimulator cells was assessed based on CTV dilution on Day 3, relative to unstimulated CAR-T cells (negative control). The percent of divided cells was normalized to the drug-free (positive) control after subtracting non-specific proliferation in the CAR-only (no tumor) negative controls for each construct (see Methods). Panels are shown for different E:T ratios of A) 1:1 B) 2:1 C) 4:1 and D) 10:1 with a CsA dose titration. Data shown reflects CAR-T cells gated on CD4. Black bars show the mean. 2-way ANOVA with Sidak post-hoc test used for statistical analysis.

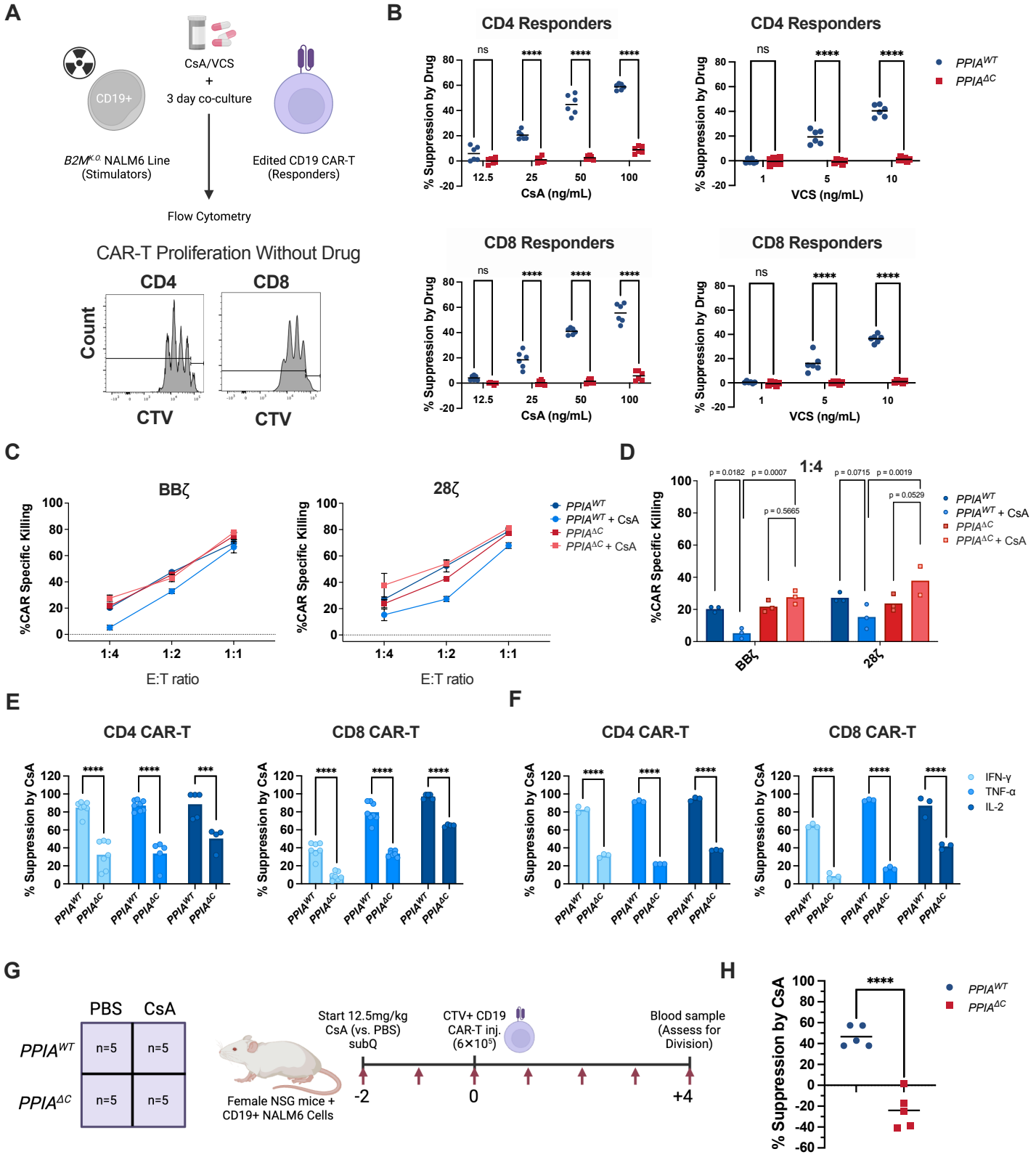

Figure 5. *PPIA*$^{\Delta C}$ CAR-T cells exhibit preserved division, cytotoxicity, and cytokine production in the presence of drug. A) Edited CD19 CAR-T cells were stimulated by β2M^{KO} NALM6 cells at a 10:1 E:T ratio. Division of CAR-T cells was assessed based on CTV dilution on Day 3, comparing to unstimulated CAR-T cells (negative control). The percent of divided cells was normalized to the drug-free (positive) control (see Methods). B) Data shown for CD4+ and CD8+ CAR-T cell division across a CsA and VCS dose titration. Black bars show the mean. n = 6 replicates. 2-way ANOVA with Sidak post-hoc test used for statistical analysis. C-D)

Cytotoxicity assay demonstrating % killing of NALM6 target cells at different effector to target (E:T) ratios after four hours of co-culture. 2-way ANOVA used for statistical analysis. E-F) To assess cytokine production, *PPIA*^{WT} or *PPIA*$^{\Delta C}$ CAR-T cells were stimulated for 4 hours in the presence of protein transport inhibitor and either E) PMA/ionomycin or F) CD19+ NALM6 cells (E:T of 2:1), and stained for intracellular IFN-γ, TNF-α, and IL-2. 100 ng/mL CsA was used for experiments. The % Suppression was calculated as described in Methods G) On Day 0, CTV labelled CD19 CAR-T cells were injected into immune deficient (NSG) mice previously inoculated with human CD19+ NALM6 cells. Mice received subcutaneous injections of CsA starting on Day -2 H) CAR-T cell division on Day +4 was assessed based on CTV dilution after gating on murine CD45-, human CD45+ cells. A two-tailed T-test was used for statistical comparison. The % suppression was calculated per Methods (n = 5 per group).

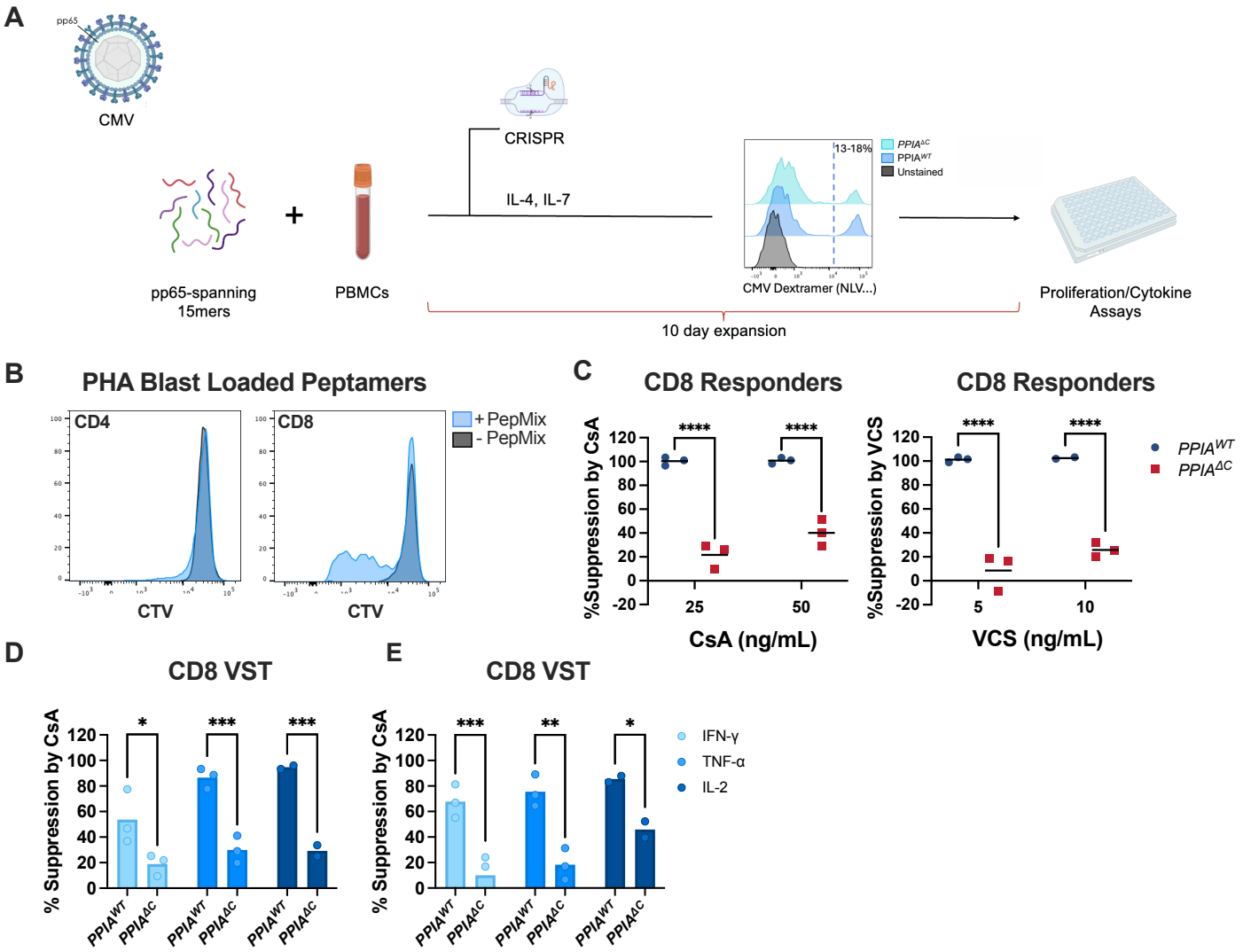

Figure 6. *PPIA*$^{\Delta C}$ VSTs exhibit preserved division and cytokine production in the presence of drug. A) Schematic for making CRISPR/Cas9 edited CMV specific VSTs from healthy donor PBMCs, of which 13-18% stained positive for HLA-A*02/NLVPMVATV after a first stimulation. B) Representative example of CD8 specific T cell proliferation after restimulation of VST culture with pp65-peptamer loaded PHA-blasts. C) % Suppression of *PPIA*^{WT} and *PPIA*$^{\Delta C}$ VST proliferation in the presence of 25 and 50 ng/ml CsA and 5 and 10 ng/ml VCS. D-E) VSTs were restimulated with (D) PMA/ionomycin or (E) PepMix and stained for intracellular cytokine production. 25 ng/mL CsA was used for these experiments. % Suppression was calculated as described in Methods. A 2-way ANOVA was used for statistical analysis.